



Partial differential equations/Numerical analysis

Wave splitting for time-dependent scattered field separation



Décomposition d'ondes pour la séparation de champs diffractés dans le domaine temporel

Marcus J. Grote^a, Marie Kray^a, Frédéric Nataf^{b,c,d}, Franck Assous^e

^a Department of Mathematics and Computer Sciences, University of Basel, Spiegelgasse 1, CH-4051 Basel, Switzerland
^b CNRS, UMR 7598, Laboratoire Jacques-Louis-Lions, 75005 Paris, France

^c UPMC Univ Paris 06, UMR 7598, Laboratoire Jacques-Louis-Lions, 75005 Paris, France

^d INRIA Rocquencourt, Alpines, BP 105, 78153 Le Chesnay cedex, France

^e Department of Computer Sciences and Mathematics, Ariel University, 40700 Ariel, Israel

ARTICLE INFO

Article history:

Received 19 December 2014

Accepted after revision 6 March 2015

Available online 4 April 2015

Presented by Haïm Brézis

ABSTRACT

Starting from classical absorbing boundary conditions, we propose a method for the separation of time-dependent scattered wave fields due to multiple sources or obstacles. In contrast to previous techniques, our method is local in space and time, deterministic, and also avoids *a priori* assumptions on the frequency spectrum of the signal.

© 2015 Académie des sciences. Published by Elsevier Masson SAS. All rights reserved.

RÉSUMÉ

À partir des conditions aux limites absorbantes classiques, nous proposons une méthode dans le domaine temporel pour la séparation des champs d'onde diffractés dus à des sources ou des obstacles multiples. Contrairement aux techniques antérieures, notre procédé est local en temps et en espace, déterministe, et ne dépend pas de connaissances *a priori* du spectre de fréquence du signal.

© 2015 Académie des sciences. Published by Elsevier Masson SAS. All rights reserved.

Version française abrégée

Lorsqu'une onde incidente éclaire un objet, le champ diffracté contient de nombreuses informations sur ses propriétés. Cependant, si les sources ne sont pas totalement connues (position ou dépendance en temps) ou que d'autres sources indésirables interfèrent, la détermination du champ diffracté par soustraction du champ incident au champ total est un problème difficile. Cette difficulté apparaît par exemple dans les techniques d'imagerie médicale utilisant des produits de contraste à microbulles [13,12].

Ce problème posé dans le domaine fréquentiel est étudié dans de nombreux articles, voir par exemple [15,6,1,4] ou [5]. Il a, en revanche, été beaucoup moins étudié dans le domaine temporel. Dans [7,8], des conditions absorbantes pour des

E-mail addresses: marcus.grote@unibas.ch (M.J. Grote), marie.kray@unibas.ch (M. Kray), nataf@ann.jussieu.fr (F. Nataf), franckassous@netscape.net (F. Assous).

problèmes de diffraction multiple ont été développées. Dans [14], le cas temporel est traité par la transformée de Fourier dans le domaine fréquentiel. Dans cette note, on présente une méthode, locale en espace et en temps, qui ne nécessite pas d'information *a priori* sur le contenu fréquentiel du signal.

On considère une onde se propageant dans un domaine contenant deux objets diffractants inclus dans des cercles disjoints S_1 et S_2 de centre C_1 et C_2 , voir Fig. 1. Le champ diffracté u , qui vérifie l'équation (1), est la somme de deux champs sortants de S_1 et de S_2 respectivement, voir (2). À partir de la donnée de u enregistrée sur une courbe Γ , on détermine de manière approchée les champs u_1 et u_2 . Pour ce faire, on introduit B_1 (resp. B_2), une condition absorbante centrée en C_1 (resp. C_2), qui fournit l'équation (4). Appliquées au champ u , elles donnent une deuxième équation (5) vérifiée par le premier terme du développement asymptotique (3) de u_1 et u_2 . En combinant ces équations avec des changements de variables adaptés, on montre que f_1 (resp. f_2), le premier terme du développement asymptotique de u_1 (resp. u_2), vérifie une équation hyperbolique du premier ordre posée sur la courbe d'observation Γ , voir (7). Cette équation est résolue par un schéma de Crank–Nicholson en temps et un schéma décentré amont en espace. La méthode est illustrée par l'exemple d'une source inconnue illuminant un objet diffractant également inconnu, voir Fig. 1. Le champ total résultant enregistré sur un arc de cercle Γ est décomposé en deux champs sortants : u_1 le champ incident et u_2 le champ diffracté par l'objet, voir Fig. 2. Les simulations numériques des champs diffractés ont été effectuées par une méthode d'éléments finis à l'aide du logiciel FreeFem++ [10]. Le principe de la méthode est valable en dimension quelconque d'espace.

1. Introduction

When an incident wave illuminates a target, be it rigid or penetrable, it generates a scattered wave that carries information about the obstacle across the host medium. Clearly, that information is readily available by subtraction of the incident wave from total field measurements. However, if the location, spatial distribution or time dependence of the original source are not precisely known, or other undesired sources interfere with the signal, the extraction of the scattered field of interest becomes non-trivial, though it remains essential for any subsequent inversion. In transcranial ultrasonic imaging, for instance, intense ultrasound pulses induce a single cavitation bubble whose collapse generates a small shock wave, then recorded by a standard ultrasound imaging array [13]; clearly, the bubble's time signature is never precisely known. Similarly, the detection of individual free-floating and targeted microbubbles of an ultrasound contrast agent is critical for quantifying the amount of bubbles in the tissue [12].

In the presence of several obstacles, each primary scattered wave will induce secondary scattered waves from all other obstacles, which again will induce further scattered waves, and so forth. Together with the incident wave, their superposition results in the measured total wave field. The inversion from the total wave field for multiple obstacles at once adds yet another layer of complexity to any algorithm for inverse scattering problems. Hence, if their superposition can be split into individual outgoing components, we can apply any algorithm for single inverse scattering to each scatterer separately. As a consequence, each isolated scattering problem will be smaller in size and less ill-conditioned than their total sum.

In the frequency domain, there is a long history of wave splitting techniques for multiple scattering problems. In his classical work, Twerksy expresses multiple scattering coefficients in terms of algebraic relations that couple the multipole coefficients of isolated scatterers—see [15] for a review. More recently, Grote and Kirsch [6] used wave splitting to derive nonreflecting boundary conditions for multiple scattering problems. Similarly, Acosta [1] formulated on-surface radiation conditions for multiple scattering. In [4], Ben Hassen, Liu and Potthast split the far-field pattern using integral based formulations to extend the point source method to inverse scattering of multiple obstacles. By combining the inverse Radon approximation with a Galerkin ansatz, Griesmaier, Hanke and Sylvester determine the convex scattering support of individual far-field components separately [5].

In the time domain, little work on inverse multiple scattering problems is available. In [7,8], nonreflecting boundary conditions for time-dependent multiple scattering were derived, which avoid the space-time integrals involved in standard integral-based formulations. By Fourier transform in the frequency domain, Potthast, Fazi and Nelson [14] devised a filter via the point source method for time-dependent source separation. Here we propose a method to determine the separate outgoing components of the incident and scattered wave fields for time-dependent multiple scattering problems. In contrast to previous work, our approach is local in space and time, deterministic, and also avoids any *a priori* assumptions on the frequency spectrum of the signal.

2. Wave splitting

We consider wave scattering from two bounded disjoint scatterers in unbounded two- or three-dimensional space. Each scatterer may contain several obstacles, inhomogeneities and nonlinearity. Next, we assume that both scatterers are well separated, that is we assume that we can surround them by two non-intersecting spheres S_1 and S_2 centered at C_1 and C_2 , respectively—see Fig. 1. In the unbounded region Ω outside the two spheres, we assume that the medium is homogeneous, isotropic, and source-free. Hence the scattered field u satisfies:

$$\frac{\partial^2 u}{\partial t^2} - c^2 \Delta u = 0 \quad \text{in } \Omega, t > 0, \tag{1}$$

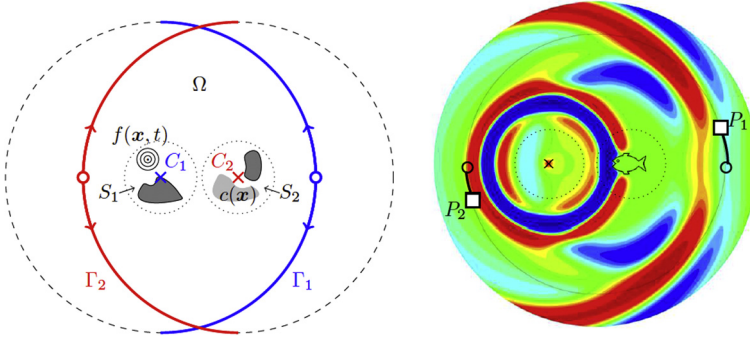


Fig. 1. (Color online.) Left: scatterer geometry and location of the observations. Right: snapshot of the total field. The incident wave originates from a point source inside S_1 , which impinges on a sound-soft fish-shaped obstacle.

Fig. 1. (Couleur en ligne.) À gauche : géométrie des diffracteurs et position des observations. À droite : instantané du champ total. Le champ incident généré par une source ponctuelle dans S_1 heurte une inclusion molle en forme de poisson.

with constant wave speed $c > 0$. Moreover, we assume that u is initially confined to the interior of $S_1 \cup S_2$ and thus vanishes throughout Ω at time $t = 0$. Therefore, it splits into two unique wave fields u_1 and u_2 [7]:

$$u = u_1 + u_2 \quad \text{in } \Omega, \quad t > 0, \quad (2)$$

where u_k is purely outgoing and satisfies (1) in the entire exterior of S_k . Each u_k is therefore determined by its time-dependent (unknown) values at S_k , $k = 1, 2$.

Now, let Γ denote a surface patch in three dimensions or a curve segment in two dimensions, not necessarily closed or connected, which lies inside Ω . Given the measured values of u on Γ , we wish to recover the entire time history of u_1 and u_2 . Since each u_k is outgoing outside S_k , it can be written as a progressive wave expansion in inverse powers of distance [3,9]. In three space dimensions, for instance, we have

$$u_k(t, r_k, \theta_k, \varphi_k) = \frac{1}{r_k} \sum_{i \geq 0} \frac{f_{k,i}(r_k - ct, \theta_k, \varphi_k)}{(r_k)^i}, \quad (3)$$

where $(r_k, \theta_k, \varphi_k)$ denote spherical coordinates centered about the origin C_k , $k = 1, 2$. Starting from (3), Bayliss and Turkel [3] derived a sequence of increasingly accurate differential operators of order m that annihilate the leading order terms in the expansion. Each operator yields an absorbing boundary condition

$$B_k[u_k] = O\left(\frac{1}{r_k^{2m+1}}\right), \quad k = 1, 2 \quad (4)$$

on Γ , where k identifies the local spherical coordinate system. Neglecting the error term in (4), we thus obtain

$$B_j[u_k] = B_j[u_k + u_j] = B_j[u], \quad j = 1, 2, k \neq j. \quad (5)$$

Since u is known on Γ , Eq. (5) yields a partial differential equation for the unknown wave field u_k . In general, it will involve tangential, normal and time derivatives. By rewriting the normal derivative as a combination of tangential and radial derivatives, and then using (4) to replace radial by time derivatives, the resulting equation will involve only tangential and time derivatives and thus be restricted to Γ . Clearly, appropriate initial and boundary conditions must be set for well-posedness. In fact, since the scattered field is initially zero in Ω , both u_k and u_j will vanish on Γ at $t = 0$.

3. Two-dimensional example

To illustrate the usefulness of the method delineated above, we now consider a two-scatterer configuration in two space dimensions. For simplicity, we let each Γ_k be a semi-circle centered at C_k of radius r_k , as shown in Fig. 1. Given the total field u at $\Gamma = \Gamma_1 \cup \Gamma_2$, we shall recover both the incident field, u_1 , and the scattered field, u_2 due to the obstacle.

In two space dimensions, the first-order Bayliss-Turkel operator is

$$B_j[u] := \frac{1}{c} \frac{\partial u}{\partial t} + \frac{\partial u}{\partial r_j} + \frac{u}{2r_j}. \quad (6)$$

Hence to derive (5), we first apply B_j to u . Then, we change coordinates from (r_j, θ_j) to (r_k, θ_k) and replace radial by time derivatives. This yields the following partial differential equation on Γ_k , where $f_{k,0}$ denotes the first term $f_{k,0}$ in the two-dimensional counterpart of (4):

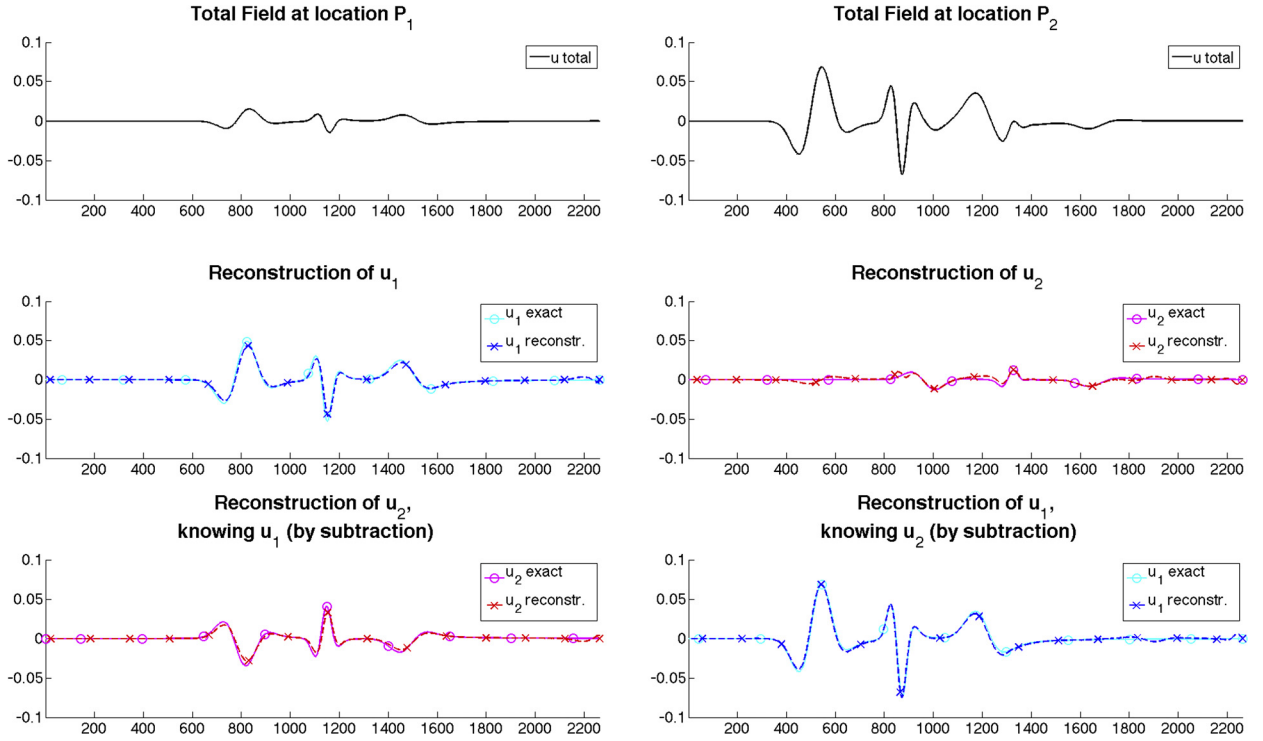


Fig. 2. (Color online.) Recovery of wave fields u_1 and u_2 from total field measurements u at location P_2 (right) and P_1 (left). Top: total field u . Middle: reconstructed field by solving (7). Bottom: second field obtained by subtraction.

Fig. 2. (Couleur en ligne.) Reconstruction des champs u_1 et u_2 à partir des mesures u à l'emplacement P_1 (colonne de droite) et l'emplacement P_2 (colonne de gauche). En haut : champ total enregistré à l'emplacement. Au milieu : champ reconstruit par séparation d'ondes. En bas : second champ calculé par soustraction.

$$\left(\alpha_k(\theta_k) \frac{\partial}{\partial t} + \beta_k(\theta_k) \frac{\partial}{\partial \theta_k} + \gamma_k(\theta_k) \right) f_k = B_j[u], \quad k, j = 1, 2, k \neq j \quad (7)$$

where

$$\begin{aligned} \alpha_k(\theta_k) &= \frac{\sqrt{r_k^2 + \ell_{k,j}^2 - 2r_k \ell_{k,j} \cos(\theta_k)} - r_k + \ell_{k,j} \cos(\theta_k)}{c \sqrt{r_k} \sqrt{r_k^2 + \ell_{k,j}^2 - 2r_k \ell_{k,j} \cos(\theta_k)}}, \\ \beta_k(\theta_k) &= \frac{\ell_{k,j} \sin(\theta_k)}{r_k \sqrt{r_k} \sqrt{r_k^2 + \ell_{k,j}^2 - 2r_k \ell_{k,j} \cos(\theta_k)}}, \\ \gamma_k(\theta_k) &= \frac{\ell_{k,j} \cos(\theta_k)}{2r_k \sqrt{r_k} \sqrt{r_k^2 + \ell_{k,j}^2 - 2r_k \ell_{k,j} \cos(\theta_k)}}, \end{aligned} \quad (8)$$

and $\ell_{k,j} := x_{C_j} - x_{C_k}$ is the signed distance between the two centers.

Since (7) is a first-order hyperbolic partial differential equation, its characteristics determine whether boundary conditions, if any, must be imposed. Consider Γ_1 , for instance, the semi-circle centered about C_1 and parameterized by $\theta_1 \in (-\pi/2, \pi/2)$ —see Fig. 1. Since $\alpha_1(\theta_1) \geq 0$ and $\gamma_1(\theta_1) \geq 0$ for $-\pi/2 \leq \theta_1 \leq \pi/2$, $\ell_{1,2} > 0$, while $\beta_1(\theta_1)$ changes sign at θ_1 , the characteristics of (7) with $k = 1, j = 2$ point to the right for θ_1 positive and to the left for θ_1 negative. Hence, Γ_1 splits into two independent quadrants at $\theta_1 = 0$, where (7) reduces to a trivial identity and thus yields the required boundary condition. At the two extremities of Γ_1 with $\theta_1 = -\pi/2, \pi/2$, however, the characteristics are outgoing and therefore no further boundary condition must be set there.

We now consider an incident wave originating from a point source, which generates a scattered field as it impinges upon a sound-soft fish-shaped inclusion. In Fig. 1, we display a snapshot of the total wave field together with the precise locations of the source, the inclusion and the observations. Given the measured total field on Γ , we wish to recover the two purely outgoing fields u_1 and u_2 at the two locations, P_1 and P_2 , shown in Fig. 1. Here, u_1 merely corresponds to the incident field, which is unknown a priori. In fact, to recover u_1 at P_1 , we only need to solve (7) on the short arc connecting

the two points $\theta_1 = 0$ and P_1 , due to the direction of the characteristics; hence, no values of u beyond that arc are needed to separate the two wave fields at P_1 .

For the numerical solution to (7), we opt for the Crank–Nicholson scheme in time and upwinding finite difference scheme in space. The source term, $B_j[u]$, on the right-hand side of (7), is computed by centered second-order differences in time and a variational formulation for the radial derivative. The source term and the synthetic measurements are computed with FREEFEM++ [10], whereas the solution to (7) is performed in Matlab to avoid any inverse crime.

In Fig. 2, we display the numerical solution at the two locations P_1 and P_2 . At P_1 , we recover f_1 from u , and then obtain f_2 by subtraction. Similarly at P_2 , we first compute f_2 and then recover f_1 by subtraction. Remarkably, even in the shadow zone where the total field essentially vanishes, our method is able to recover both outgoing components.

Although we have illustrated our method with only two superposed scalar wave fields, it not only extends to arbitrarily many, but also to vector-valued wave equations from electromagnetics and elasticity. Since shear and compressional waves propagate at different speeds, radiation boundary conditions [11] probably enable the separation of the two elastic wave fields and would thereby improve full-field elasticity imaging [2]. When higher-order absorbing conditions are used, higher-order corrections in (3) can be determined, if needed.

References

- [1] S. Acosta, On-surface radiation condition for multiple scattering of waves, *Comput. Methods Appl. Mech. Eng.* 283 (2015) 1296–1309.
- [2] H. Ammari, E. Bretin, J. Garnier, W. Jing, H. Kang, A. Wahab, Localization, stability, and resolution of topological derivative based imaging functionals in elasticity, *SIAM J. Imaging Sci.* 6 (4) (2013) 2174–2212.
- [3] A. Bayliss, E. Turkel, Radiation boundary conditions for wave-like equations, *Commun. Pure Appl. Math.* 33 (6) (1980) 707–725.
- [4] F. Ben Hassen, J. Liu, R. Potthast, On source analysis by wave splitting with applications in inverse scattering of multiple obstacles, *J. Comput. Math.* 25 (3) (2007) 266–281.
- [5] R. Griesmaier, M. Hanke, J. Sylvester, Far field splitting for the Helmholtz equation, *SIAM J. Numer. Anal.* 52 (1) (2014) 343–362.
- [6] M.J. Grote, C. Kirsch, Dirichlet-to-Neumann boundary conditions for multiple scattering problems, *J. Comput. Phys.* 201 (2) (2004) 630–650.
- [7] M.J. Grote, C. Kirsch, Nonreflecting boundary condition for time-dependent multiple scattering, *J. Comput. Phys.* 221 (1) (2007) 41–67.
- [8] M.J. Grote, I. Sim, Local nonreflecting boundary condition for time-dependent multiple scattering, *J. Comput. Phys.* 230 (8) (2011) 3135–3154.
- [9] T. Hagstrom, S.I. Hariharan, A formulation of asymptotic and exact boundary conditions using local operators, *Appl. Numer. Math.* 27 (1998) 403–416.
- [10] F. Hecht, New development in FreeFem++, *J. Numer. Math.* 20 (3–4) (2012) 251–265.
- [11] R.L. Higdon, Radiation boundary conditions for elastic wave propagation, *SIAM J. Numer. Anal.* 27 (4) (1990) 831–869.
- [12] A.L. Klibanov, P.T. Rasche, M.S. Hughes, J.K. Wojdyla, K.P. Galen, J.H.J. Wible, G.H. Brandenburger, Detection of individual microbubbles of ultrasound contrast agents: imaging of free-floating and targeted bubbles, *Invest. Radiol.* 39 (3) (2004) 187–195.
- [13] M. Pernot, G. Montaldo, M. Tanter, M. Fink, ‘Ultrasound stars’ for time reversal focusing using induced cavitation bubbles, *Appl. Phys. Lett.* 88 (3) (2006) 034102.
- [14] R. Potthast, F.M. Fazi, P.A. Nelson, Source splitting via the point source method, *Inverse Probl.* 26 (4) (2010) 045002.
- [15] V. Twersky, On multiple scattering of waves, *J. Res. Natl. Bur. Stand.* 64D (1960) 715–730.